Cellular and Molecular Biology
E-ISSN : 1165-158X / P-ISSN : 0145-5680
www.cellmolbiol.org

Original Research

Validation of an air/liquid interface device for TiO_2 nanoparticle toxicity assessment on NR8383 cells: preliminary results

Mélanie M Leroux[#], Zahra Doumandji[#], Laëtitia Chézeau, Romain Hocquel, Luc Ferrari, Olivier Joubert, Phèdre Rihn, Bertrand H Rihn[*]

Institut Jean-Lamour, UMR 7198 CNRS, Université de Lorraine, F-54506 Vandœuvre-lès-Nancy, Cedex, France

[*]**Correspondence to:** bertrand.rihn@univ-lorraine.fr

[#]Both contributed equally to the work.

Received February 18, 2020; **Accepted** June 15, 2020; **Published** September 30, 2020

Doi: http://dx.doi.org/10.14715/cmb/2020.66.6.20

Abstract: Investigations on adverse biological effects of nanoparticles (NP) are performed usually either *in vivo* on rodents or *in vitro* under submerged conditions where NP are in suspension into cell culture media. However, sedimentation of NP *in vitro* is a continuous process and to assess the exact deposited cellular dose remains difficult, as the cellular internal dose is a function of time. Moreover, the cellular responses to NP under submerged culture conditions or by exposing rodents by nose-only to NP aerosols might differ from those observed at physiological settings at the air-liquid interface (ALI). Rat alveolar NR8383 macrophages were exposed to aerosols at the air-liquid interface. We studied TiO_2 NM105, a mixture of anatase and rutile. NR8383 cells were exposed to a single dose of 3.0 cm^2/cm^2 of TiO_2 aerosol. Following RNA extraction, transcriptome allowing full coverage of the rat genome was performed, and differentially expressed genes were retrieved. Their products were analyzed for functions and interaction with String DB. Only 126 genes were differentially expressed and 98 were recognized by String DB and give us the gene expression signature of exposed rat alveolar NR8383 macrophages. Among them, 13 display relationships at a high confidence level and the ten most differentially expressed compared to unexposed cells were: *Chac1*, *Ccl4*, *Zfp668*, *Fam129b*, *Nab2*, *Txnip*, *Id1*, *Cdc42ep3*, *Dusp6* and *Myc*, ranked from the most overexpressed to the most under-expressed. Some of them were previously described as over or under-expressed in NP exposed cell systems. We validated in our laboratory an easy-to-use device and a physiological relevant paradigm for studying the effects of cell exposure to TiO_2. *Ccl4* gene expression seems to be a positive marker of exposure evidenced as well as *in vivo* or in both *in vitro* conditions.

Key words: Air-liquid interface (ALI); Anatase (1317-70-0); Rutile (98084-96-9); NR8383; Microarray; Chac1; Ccl4; Zfp668; Fam129b; Nab2; Txnip; Id1; Cdc42ep3; Dusp6; Myc.

Introduction

Today, nano-particles and nano-sensors provide many applications and services in human life (1, 2). Titanium dioxide (TiO_2) is among the most widely used and produced nanomaterials worldwide especially in coating paints, food products, toothpaste, pharmaceuticals, and cosmetics including sunscreens (3). More than 200,000 tons of TiO_2 NP were produced worldwide in 2015, and if workers are exposed by inhalation, consumers may be exposed mainly by the skin and gastrointestinal tract routes (4, 5).

NM105 is an NP mixture of both main crystallographic forms of TiO_2, anatase and rutile (6). Recently some of us (LC, OJ & BHR) published a well-designed *in vivo* study on Fischer 344 rats exposed by nose-only inhalation to 10 mg/m^3 of a TiO_2 nanostructured aerosol. Lung samples showed a strong inflammatory response up to 3 post-exposure days, which decreased over time as evidenced by recent transcriptomic and proteomic studies in rat lung (7, 8). We used the same species of NP (NM105) in exposing rat NR8383, a rat alveolar macrophage cell line in order to compare both *in vivo* and *in vitro* obtained transcriptomes. By the way ECVAM and EU policy prompt scientists to use *in vitro* paradigms in application to the 3R rule.

In a first-tier we try to mimic lung exposure in an ALI model by exposing macrophages directly to NM105 aerosol to validate our approach, namely the aim of this study. In second-tier transcriptomes of submerged cultures were compared to those we obtain with ALI exposure. For a third tier, we plan to culture NR8383 cells together with rat pneumocytes and to compare transcriptomes of rat lung and co-cultured cells. Co-culture in ALI systems seems a more relevant model from a physiological point of view compared to the co-cultures of submerged cells, a more popular *in vitro* model. ALI models were used recently to evaluate the effect of cigarette smokes (9) and diesel exhausts (10). Several groups are now using this model for studying responses to NP exposure, either silica (11), either TiO_2 and CeO_2 (12) or CuO (13) in Vitrocell® ALI device with either A549 cells or nasal epithelial cells from donors.

Materials and Methods

Characterization of TiO_2 nanoparticles

For the present study, we used the TiO_2 nanomaterial NM 105 (CAS 13463-67-7), namely a mixture of anatase (1317-70-0) and rutile (98084-96-9), obtained

from Join Research Center (European Chemical Bureau, Ispra, Italy). Hydrodynamic diameter average (*Z*-average), polydispersity index, and zeta potential of the nanomaterials were performed with Malvern Nano Zetasizer (Malvern Inc., Worcs, UK) at a 200 µg/ml (w/v) concentration in water. The specific surface area and zeta potentials were 51 m^2/g and +11.1 ± 0.7 mV respectively.

Z-average was 128.0 ± 4.7 nm with a polydispersity index of 0.15.

Cell culture and exposure to NM105 aerosol in an ALI system

NR8383 rat alveolar macrophages were purchased from American Type Culture Collection (ATCC® CRL2192™, Manassas, USA). Cells were cultured in Dulbecco's Modified Eagle Medium, high glucose, supplemented with 15% fetal bovine serum, 100 U/ml penicillin and 100 µg/ml streptomycin, 4 mM L-glutamine and 0.25 µg/mL of amphotericin B. All chemicals were purchased at Sigma-Aldrich (St. Louis; USA). Cells were cultured at 37°C in a humidified chamber with 5 % CO_2 and passaged every 3 d. At the beginning of the experimentation, 300,000 cells were deposited in a transwell insert onto an Air-Liquid Interface device (Vitrocell Cloud 6™, Waldkirch, Germany). Cells were cultured onto transwell inserts placed into a culture well with supplied medium at basal part only and aerosol was spread at the apical part. Twenty-four h later, porcine surfactant, purified according to Taeusch *et al.* (14), and a generous gift from J Perez-Gil (Faculty of Biology, Complutense University, Madrid, Spain), was aerosolized onto cells in order to reduce the surface tension of the air-liquid interface at a dose of 2.4 mg (dissolved in 61 µL) just before exposing cells to NP.

To achieve a deposited dose of 3 cm^2 of nanomaterial for 1 cm^2 of exposed cells, 170 µg of NM105 NP was dissolved in of 114 µL of ultrapure water and aerosolized by nebulization into the chamber. Following 4 h, cells were removed in order to extract RNA for transcriptome analysis. One well of the ALI system allowed us to measure the weight of deposited NM105 to control the delivered dose to cells thanks to a quartz microbalance. The five remaining wells were used as replicates for further transcriptome and RT-qPCR studies.

RNA Extraction

RNA extraction was performed as previously described (15). Briefly, following NR8383 cells exposure to a 3.0 cm^2/cm^2 of NM105 for 4 h, membranes were disrupted by adding 1 mL of Trizol™ Extraction Reagent (Omega Bio-Tek, Guangzhou, China), and 200 µL of chloroform (Carlo Erba reagents, Rouen, France). Following centrifugation and precipitation with 500 µL of isopropanol (Carlo Erba reagents, France), the precipitates were washed with ethanol/water (80%/20%) and incubated for 10 min at 60°C to remove ethanol and further dissolved in 35 µL RNase-free water. All RNA samples were of high purity and integrity (data not shown), as demonstrated by (*i*) A260/A280 ratios between ranking 2.0 and 2.2 as measured using a BioSpec-nano Spectrophotometer (Shimadzu, Marne-la-Vallée, France), and (*ii*) RNA integrity number that was above 9.0 as checked by RNA 6000 Nano Reagents Kit using Bioanalyzer™ 2100 (Agilent Technologies, Les Ulis, France).

Microarray and hybridization

The microarray was prepared as previously described (15). One hundred ng of each RNA sample was labeled with cyanine 3-CTP with reverse transcriptase (EC. 2.2.2.49) using Low Input Quick Amp Labeling kits (Agilent Technologies, France) according to the manufacturer's protocol. Labeled cRNAs were purified and hybridized overnight onto Agilent G4853A SurePrint G3 Rat version 2 GE 8*60K microarrays (Agilent Technologies, France) that allow full coverage of rat transcriptome. Microarray slides were scanned on an Agilent G2505C microarray scanner at 3 µm resolution.

Data analysis

Data were analyzed using two open-access tools: DAVID Functional Annotation Bioinformatics Microarray analysis (https://david.ncifcrf.gov/) and String (https://string-db.org/), that forms functional protein association networks. Only genes with behaving a fold change (FC) expression level > | 1.5| and p > 0.05 were incorporated in strong analysis for which we set a high confidence level (p>0.7) and Kmean of 3. Two KEGG pathways were enriched in using those clustering conditions.

Results and discussion

One hundred twenty-six genes of the whole rat genome were differentially expressed (FC> |1.5|) in exposed cells. Among them, 98 were recognized and analyzed by String DB. Among them, 43 were uncharacterized LOC, FAM or Expressed Sequences Tags.

Figure 1 shows 13 proteins behaving strong relationships through known interactions either from curated databases or experimentally determined and predicted interaction. String DB allows also to retrieve their interplay in Kyoto Encyclopedia Genes and Genomes

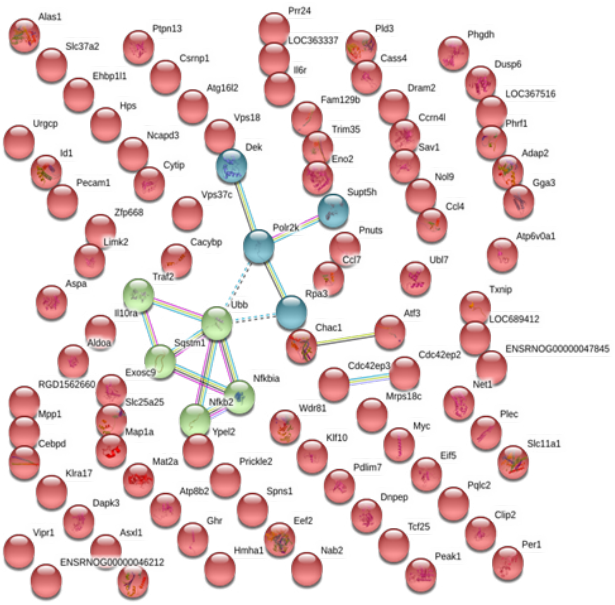

Figure 1. String DB network and signature of the 98 proteins where the gene has been differentially expressed following exposure to NM105. Only 13 proteins (13%) display a known relationship in 3 networks.

(KEGG). At the high level of confidence two KEGG enrichments are evidenced:

(*i*) 'Epstein-Barr virus infection', with the involvement of 6 genes: *Il10ra*, *Myc*, *Nfkb2*, *Nfkbia*, *Polr2k* and *Traf2*, three of which are also involved in the other gene clusters, namely (*ii*) 'NF-kappa B signaling pathway': *Ccl4*, *Nfkb2*, *Nfkbia* and *Traf2*. It should be noted that both clusters were previously evidenced following exposure of (*i*) a primary human breast cell line (HMEC 184) and THP-1 monocytes to 25 µg/mL polymeric nanoparticles (16, 17), (*ii*) THP-1 cells to 0.29 cm^2/cm^2 ZnO NP (or NM110, 18) and (*iii*) NR8383 cells to 0.58 cm^2/cm^2 of the same ZnO NP (19).

Thus it is now well known that NP induces in immune cells like monocytes and polynuclear cells, activation of oxidative stress that is mediated either by NfκB or NRF2 pathways. Moreover, a previous study pointed out that polymeric Eudragit™ NP activates also numerous genes involved in virus/macrophage interaction: as virus and NP have similar size, one can hypothesize that even entry mechanism is different, virus involves similar defense mechanisms in macrophage, especially when they are hydrolyzed in phagolysosomes (16).

It is striking to note that fewer genes are shown to be differentially expressed (DE) following an ALI exposure as compared to DE genes following submerged *in vitro* exposure; 126 vs 360 (Table I). Of course, we compare two different NP - TiO_2 and ZnO - the first a dose of 3.0 cm^2/cm^2 and the latter for a dose more than 10 times less, namely 0.29 cm^2/cm^2 and two different cell lines, the first NR8383 rat macrophages and the latter THP-1 human monocytes (18). By the way, NR8383 exposed to subtoxic doses of 0.58 cm^2/cm^2 of ZnO NP, displayed 985 differentially expressed genes using a similar FC cutoff (19). To date, we do not have analyzed the data of the submerged experiment, namely *in vitro* TiO_2 exposure of NR8383 cells. However, the present transcriptome will be compared further to *in vivo* (7) and *in vitro* data (data not shown).

Interestingly less significant impacts in cytotoxicity and oxidative stress have already been observed by comparing ALI-exposed vs submerged cells: this fact was noted for both viability and oxidative stress levels as assayed respectively by Alamar® blue test and dichlorofluorescein (DCF) to measure intracellular Reactive Oxygen Species (12). This may be explained by a lower expression level of genes involved in those functions. Unfortunately, no transcriptomic data were available in the latter study. Another group emphasizes the crucial role of temperature and relative humidity by preventing cell desiccation; in our device, both parameters were controlled allowing comparison of exposure conditions and inter-laboratory variations (20). Similarly, Panas *et al.* (11) obtained higher toxicity effect in terms of (*i*) LDH release, (*ii*) IL-8 production and (*iii*) COX-2 protein expression by exposing A549 submerged pneumocytes to 15.6 µg/cm^2 of 50 nm sized-SiO_2 NP compared to 117 µg/cm^2 of the same NP in ALI exposed cells. For submerged conditions, particles continuously settle down and induce a constant reactivity of cells increasing their sensitivity: this is not the case for ALI exposed cells where cells are exposed to a unique 'shoot' of particles. In contrast, it should be mentioned that cytotoxicity of amine-functionalized polystyrene nanoparticles was significantly higher when applied as an aerosol on cell-cultured in air-liquid interface culture at a dose of 31 µg/cm^2 compared with nanoparticle suspensions tested in submersed culture (62 µg/cm^2) as shown by Fröhlich *et al.* (21).

We were also interested in the five more over- and under-expressed genes (Table 2). Chronic exposure of rodents to TiO_2 NP was suspected to induce renal fibrosis through a mechanism involving gene activation of (*i*) the *Wnt* series, (*ii*) *Estrogen Receptor* and (*iii*) c-*Myc* pathways by Hong *et al.* (22) who evidenced significant c-*Myc* activation. In another experimentation conducted

Table 1. Comparison of recent experimentations involving metallic NP.

NP	cell system	Dose (cm^2/cm^2)	Number	Experiment	Reference
TiO_2	NR8383	1.90	126	ALI	Present study
ZnO	NR8383	0.58	985	*In vitro*	19
ZnO	THP-1	0.29	360	*In vitro*	18

Table 2. Five most under- and overexpressed genes: symbols, FC, description and main biochemical action of product and related publications.

Myc	-3.0	Myc proto-oncogene protein	Transcription factor that binds DNA to activate transcription of growth-related genes	22, 23
Dusp6	-2.3	Dual specificity protein phosphatase 6	Inactivates MAP kinases	24
Cdc42ep3	-2.3	CDC42 effector protein 3	Rho GTPase binding; role in actin filament binding	NA*
Id1	-2.2	DNA-binding protein inhibitor ID-1	Transcriptional regulator which negatively regulates the basic helix-loop-helix (bHLH) transcription	25
Txnip	-2.2	Thioredoxin-interacting protein	May act as an oxidative stress mediator by inhibiting thioredoxin activity or by limiting its bioavailability	26, 27
Nab2	1.9	Ngfi-A binding protein 2	-	NA
Fam129b	1.9	Niban-like protein 1	May play a role in apoptosis suppression	NA
Zfp668	2.1	Zinc finger protein 668		NA
Ccl4	2.1	C-C motif chemokine 4	Monokine with inflammatory and chemokinetic properties	28, 29
Chac1	2.3	Glutathione-specific gamma-glutamylcyclotransferase 1	Catalyzes the cleavage of glutathione into 5-oxo-L- proline and a Cys-Gly dipeptide	30

NA*: not available as far as our knowledge.

by Gao *et al.* (23), the c-myc protein was shown overexpressed in lymph nodes of mice exposed by intradermal injection with nanosized TiO_2. It is difficult to compare with our data, as those experiment designs are very different from the one chosen in our study. Moreover, Diao *et al.* (24) used poly (ethylene glycol)-b-poly(D, L)-lactide also called PEG-PLA) nanoparticles for silencing genes involved in myocardial proliferation and as a side effect, the *Dusp6* gene was also inhibited by PEG-PLA nanoparticles.

As for Id genes, magnetite NP exerts their significant underexpression, especially Id1 whose expression was known decreased in several immune cells lines (RAW264.7, THP-1 and HL7702) but also in the liver as related *in vivo* following exposure to 5 mg/kg body weight of magnetite NP by Zou *et al.* (25). Thioredoxin plays a central role in cellular redox balance and following oxidative stress; this [2Fe-2S] protein is dissociated from the thioredoxin-interacting protein ('txnip') that inhibits its function and activate in turn the NLRP3 inflammasome complex and finally induce IL-1β production. Lunov *et al.* (26) and Thummabancha *et al.* (27) have demonstrated such a pathway induced in respectively human macrophage exposed to amino-functionalized polystyrene nanoparticles and in zebrafish exposed to 100 mg/kg silver NP. In our study, we did not evidence any overexpression of the NLRP3 inflammasome complex, but one can assume that less inhibition of thioredoxin by txnip favored thioredoxin activity in resolving induced oxidative stress.

As for Ccl4 belonging to the large chemokine family, two recent studies, as well *in vitro* and *in vivo*, described its overexpression: (*i*) NR8383 rat alveolar macrophages were challenged with nanosized titanium dioxide particles (rutile and anatase) for 16 h and, (*ii*) mice were exposed to 5 mg/kg to 50 mg/kg of TiO_2 by a single intratracheal instillation (28, 29). In both cases, *Ccl4* was overexpressed and was considered as a good marker of inflammation.

In another study, 10 mg/kg body weight of TiO_2 NP was administered to the mice per os for 90 d and microarray was performed on immune cells by Sheng *et al.* (30). This group evidenced also *Chac1* overexpression as an immune/inflammatory response to TiO_2 exposure. Reduced glutathione is the most anti-oxidant defense mechanism in cells where its concentration reaches 10 mM and chac1 is an critical enzyme for its metabolism and recycling.

Finally, in our study we validated a recently manufactured device mimicking air exposure of NP in a realistic situation relevant for inhalation compared to submerged *in vitro* systems with or without transwell. We studied the molecular signature of a single exposure of NR8383 cells to a nanosized aerosol of TiO_2. We compare our results with those retrieved in the biomedical literature and we found relevant data to validate our paradigm. Previously we published the lung transcriptome (7) and the broncho-alveolar liquid proteome (8) of rats exposed to the same aerosol in order to compare the gene expression profiles obtained from both paradigms.

Some genes or clusters of genes are common like certain chemokines however the study is still ongoing as well as the comparison of genes expressed in submerged NR8383 cells at the same dose, namely 3.0 cm^2/cm^2. Furthermore, some of the genes like *Cdc42ep2*, *Nab2*, *Zfp668* and *Fam129b* evidenced in our study were never associated with NP exposure before: this device may be a promising tool to study the complex interplay of target cells and NP and in addition to replace advantageously *in vivo* experiments.

Acknowledgements

Funding information: This work has received funding from the European Union's Horizon 2020 research and innovation program under grant agreement No. 686098.

References

1. Moradi S, Khaledian S, Abdoli M, Shahlaei M, Kahrizi D. Nanobiosensors in cellular and molecular biology. Cell Mol Biol 2018; 64(2): 85-90.

2. Darvishi E, Kahrizi D, Arkan E. Comparison of different properties of zinc oxide nanoparticles synthesized by the green (using *Juglans regia L*. leaf extract) and chemical methods. J Mol Liquids 2019; 286, 110831.

3. Luo ZX, Wang ZH, Xu B, Sarakiotis IL, Du Laing G, Yan CZ. Measurement and characterization of engineered titanium dioxide nanoparticles in the environment. Journal of Zhejiang University Science A. 2014; 15(8):593-605.

4. Blanchart P. Extraction, Properties and Applications of Titania. Industrial Chemistry of Oxides for Emerging Applications. 2018; 255-309.

5. Youssef Z. TiO_2 Nanoparticles Coupled To Photosensitizers For Applications In Photocatalysis And Photodynamic Therapy. 2017. Philosophical Doctorate dissertation, Université de Lorraine/Université libanaise.

6. Rasmussen K, Mas J, *et al.* Titanium Dioxide, NM-100, NM-101, NM-102, NM-103, NM-104, NM-105: Characterisation and Physico-Chemical Properties, JRC Repository: NM-series of Representative Manufactured Nanomaterials. 208 pp, ISBN 978-92-79-38189-8, Luxembourg, 2014.

7. Chézeau L, Sébillaud S, Safar R, Seidel C, Dembélé D, Lorcin M, Langlais C, Grossmann S, Nunge H, Michaux S, Dubois-Pot-Schneider H, Rihn B, Joubert O, Binet S, Cosnier F, Gaté L. Short- and long-term gene expression profiles induced by inhaled TiO_2 nanostructured aerosol in rat lung. Toxicol Appl Pharmacol. 2018; 356:54-64.

8. Chézeau L, Kohlstaedt LA, Le Faou A, Cosnier F, Rihn B, Gaté L. Proteomic analysis of bronchoalveolar lavage fluid in rat exposed to TiO(2) nanostructured aerosol by inhalation. J Proteomics. 2019; 207:103451.

9. Fowler K, Fields W, Hargreaves V, Reeve L, Bombick B. Development, qualification, validation and application of the Ames test using a Vitrocell VC10® smoke exposure system. Toxicol Rep. 2018; 5:542-551.

10. Keyser BM, Leverette R, Fowler K, Fields W, Hargreaves V, Reeve L, Bombick B. Development of a quantitative method for assessment of dose in *in vitro* evaluations using a Vitrocell® VC10® smoke exposure system. Toxicol In Vitro. 2019; 56:19-29.

11. Panas A, Comouth A, Saathoff H, Leisner T, Al-Rawi M, Simon M, Seemann G, Dössel O, Mülhopt S, Paur HR, Fritsch-Decker S, Weiss C, Diabaté S. Silica nanoparticles are less toxic to human lung cells when deposited at the air-liquid interface compared to conventional submerged exposure. Beilstein J Nanotechnol. 2014; 5:1590-1602.

12. Loret T, Peyret E, Dubreuil M, Aguerre-Chariol O, Bressot C, le Bihan O, Amodeo T, Trouiller B, Braun A, Egles C, Lacroix G. Air-

liquid interface exposure to aerosols of poorly soluble nanomaterials induces different biological activation levels compared to exposure to suspensions. Part Fibre Toxicol. 2016; 13(1):58.
13. Kooter IM, Gröllers-Mulderij M, Duistermaat E, Kuper F, Schoen ED. Factors of concern in a human 3D cellular airway model exposed to aerosols of nanoparticles. Toxicol In Vitro. 2017; 44:339-348.
14. Taeusch HW, Bernardino de la Serna J, Perez-Gil J, Alonso C, Zasadzinski JA. Inactivation of pulmonary surfactant due to serum-inhibited adsorption and reversal by hydrophilic polymers: experimental. Biophys J. 2005; 89(3):1769-79.
15. Nahle S, Safar R, Grandemange S, Foliguet B, Lovera-Leroux M, Doumandji Z, Le Faou A, Joubert O, Rihn B, Ferrari L. Single wall and multiwall carbon nanotubes induce different toxicological responses in rat alveolar macrophages. J Appl Toxicol. 2019; 39(5):764-772.
16. Hussien R, Rihn BH, Eidi H, Ronzani C, Joubert O, Ferrari L, Vazquez O, Kaufer D, Brooks GA. Unique growth pattern of human mammary epithelial cells induced by polymeric nanoparticles. Physiol Rep. 2013; 1(4):e00027. doi: 10.1002/phy2.27.
17. Ronzani C, Safar R, Diab R, Chevrier J, Paoli J, Abdel-Wahhab MA, Le Faou A, Rihn BH, Joubert O. Viability and gene expression responses to polymeric nanoparticles in human and rat cells. Cell Biol Toxicol. 2014; 30(3):137-46.
18. Safar R, Doumandji Z, Saidou T, Ferrari L, Nahle S, Rihn BH, Joubert O. Cytotoxicity and global transcriptional responses induced by zinc oxide nanoparticles NM 110 in PMA-differentiated THP-1 cells. Toxicol Lett. 2019; 308:65-73.
19. Doumandji Z, Safar R, Lovera-Leroux M, Nahle S, Hilary C, Gomez D, Rihn BH, Ferrari L, Joubert O. Protein and lipid homeostasis altered in rat macrophages after exposure to metallic oxide nanoparticles. Cell Biol Toxicol. 2019; doi:10.1007/s10565-019-09484-6.
20. Zavala J, Greenan R, Krantz QT, DeMarini DM, Higuchi M, Gilmour MI, White PA. Regulating temperature and relative humidity in air-liquid interface in vitro systems eliminates cytotoxicity resulting from control air exposures. Toxicol Res (Camb). 2017; 6(4):448-459. doi: 10.1039/c7tx00109f. eCollection 2017 Jul 1. PMID: 30090513
21. Fröhlich E, Bonstingl G, Höfler A, Meindl C, Leitinger G, Pieber TR, Roblegg E. Comparison of two *in vitro* systems to assess cellular effects of nanoparticles-containing aerosols. Toxicol In Vitro. 2013; 27(1):409-17.
22. Hong F, Hong J, Wang L, Zhou Y, Liu D, Xu B, Yu X, Sheng L. Chronic exposure to nanoparticulate TiO2 causes renal fibrosis involving activation of the Wnt pathway in mouse kidney. J Agric Food Chem. 2015; 63(5):1639-47.
23. Gao Y, Gopee NV, Howard PC, Yu LR. Proteomic analysis of early response lymph node proteins in mice treated with titanium dioxide nanoparticles. J Proteomics. 2011; 74(12):2745-59.
24. Diao J, Wang H, Chang N, Zhou XH, Zhu X, Wang J, Xiong JW. PEG- PLA nanoparticles facilitate siRNA knockdown in adult zebrafish heart. Dev Biol. 2015; 406(2):196-202.
25. Zou J, Wang X, Zhang L, Wang J. Iron nanoparticles significantly affect the *in vitro* and *in vivo* expression of *Id* genes. Chem Res Toxicol. 2015; 28(3):373-83.
26. Lunov O, Syrovets T, Loos C, Nienhaus GU, Mailänder V, Landfester K, Rouis M, Simmet T. Amino-functionalized polystyrene nanoparticles activate the NLRP3 inflammasome in human macrophages. ACS Nano. 2011; 5(12):9648-57.
27. Thummabancha K, Onparn N, Srisapoome P. Molecular characterization and expression analyses of cDNAs encoding the thioredoxin-interacting protein and selenoprotein P genes and histological changes in Nile tilapia (*Oreochromis niloticus*) in response to silver nanoparticle exposure. Gene. 2016; 577(2):161-73.
28. Schremmer I, Brik A, Weber DG, Rosenkranz N, Rostek A, Loza K, Brüning T, Johnen G, Epple M, Bünger J, Westphal GA. Kinetics of chemotaxis, cytokine, and chemokine release of NR8383 macrophages after exposure to inflammatory and inert granular insoluble particles. Toxicol Lett. 2016; 263:68-75.
29 Park EJ, Yoon J, Choi K, Yi J, Park K. Induction of chronic inflammation in mice treated with titanium dioxide nanoparticles by intratracheal instillation. Toxicology. 2009; 260(1-3):37-46.
30. Sheng L, Wang L, Sang X, Zhao X, Hong J, Cheng S, Yu X, Liu D, Xu B, Hu R, SunQ, Cheng J, Cheng Z, Gui S, Hong F. Nano-sized titanium dioxide-induced splenic toxicity: a biological pathway explored using microarray technology. J Hazard Mater. 2014; 278:180-8.